Muon spin relaxation studies of the frustrated quasi-two-dimensional square-lattice spin system Cu(Cl,Br)La(Nb,Ta)$_2$O$_7$: Evolution from spin-gap to antiferromagnetic state

Y. J. Uemura,[1,*] A. A. Aczel,[2] Y. Ajiro,[3] J. P. Carlo,[1] T. Goko,[1,4] D. A. Goldfeld,[1] A. Kitada,[3] G. M. Luke,[2]
G. J. MacDougall,[2] I. G. Mihailescu,[1] J. A. Rodriguez,[2] P. L. Russo,[1] Y. Tsujimoto,[3] C. R. Wiebe,[5] T. J. Williams,[2]
T. Yamamoto,[3] K. Yoshimura,[3] and H. Kageyama[3,*]

[1]*Department of Physics, Columbia University, New York, New York 10027, USA*
[2]*Department of Physics and Astronomy, McMaster University, Hamilton, Ontario, Canada L8S 4M1*
[3]*Department of Chemistry, Kyoto University, Kyoto 606-8502, Japan*
[4]*TRIUMF, Vancouver, British Columbia, Canada V6T 2A3*
[5]*Department of Physics, Florida State University, Tallahassee, Florida 32310, USA*
(Received 16 February 2009; published 13 November 2009)

We report muon spin relaxation (μSR) and magnetic-susceptibility measurements on Cu(Cl,Br)La(Nb,Ta)$_2$O$_7$, which demonstrate: (a) the absence of static magnetism in (CuCl)LaNb$_2$O$_7$ down to 15 mK confirming a spin-gapped ground state; (b) phase separation between partial volumes with a spin-gap and static magnetism in (CuCl)La(Nb,Ta)$_2$O$_7$; (c) history-dependent magnetization in the (Nb,Ta) and (Cl,Br) substitution systems; (d) a uniform long-range collinear antiferromagnetic state in (CuBr)LaNb$_2$O$_7$; and (e) a decrease in Néel temperature with decreasing Br concentration x in Cu(Cl$_{1-x}$Br$_x$)LaNb$_2$O$_7$ with no change in the ordered Cu moment size for $0.33 \leq x \leq 1$. Together with several other μSR studies of quantum phase transitions in geometrically frustrated spin systems, the present results reveal that the evolution from a spin-gap to a magnetically ordered state is often associated with phase separation and/or a first-order phase transition.

I. INTRODUCTION

Modern studies of quantum phase transitions (QPTs) seek novel features of ground states near phase boundaries. In a narrow range of J_2/J_1 ratios of square-lattice spin systems, geometrical frustration of the nearest-neighbor (J_1) and next-nearest-neighbor (J_2) exchange interactions is expected to yield a spin-gap state. Recent synthesis of a new square-lattice system (CuCl)LaNb$_2$O$_7$ brought the first long-awaited system that might help to elucidate this hypothesis and the associated QPT. In this paper, we report muon spin relaxation (μSR) and low-field susceptibility studies of this system and relevant compounds obtained by (Cl,Br) and (Nb,Ta) substitutions.

Unlike thermal phase transitions that represent changes in systems as a function of temperature, studies of QPTs follow the evolution of ground states across phase boundaries at $T \rightarrow 0$ by varying, for example, chemical composition or pressure as a tuning parameter. Recent experimental studies revealed unexpected features of QPTs, such as first-orderlike behavior, phase separation, and slow spin fluctuations at boundaries of magnetically ordered and paramagnetic states in itinerant electron magnets. We refer to MnSi (Refs. 1–3) and (Sr,Ca)RuO$_3$,[3] which are metallic systems without spin frustration. Phase separation has also been found between the stripe spin-charge ordered state and the superconducting states without static magnetism in high-T_c cuprate systems[4–6] involving holes doped in antiferromagnetic CuO$_2$ planes. It is interesting to compare these results to QPTs of insulating and geometrically frustrated spin systems (GFSS) (Refs. 7 and 8) at boundaries between magnetically ordered states and spin-gap/spin-liquid states realized without static magnetism.

GFSS on triangular or Kagomé lattices exclusively involve antiferromagnetic nearest-neighbor interactions in hex-

agonal geometry. In contrast, the two-dimensional (2D) square-lattice J_1-J_2 system is unique in its underlying square-lattice geometry as well as the possible involvement of ferromagnetic interactions. Several compounds of vanadium oxide,[9,10] synthesized in the early search for spin-gapped J_1-J_2 materials, unfortunately showed magnetic order at low temperatures (2.1–3.5 K). As illustrated in Fig. 1(c), the J_2/J_1 ratios of these systems, estimated from magnetic susceptibility, narrowly missed the region predicted for formation of a singlet ground state with a spin gap.[12,13]

In 2005, Kageyama *et al.*[11] succeeded in synthesizing a spin-gap candidate J_1-J_2 system (CuCl)LaNb$_2$O$_7$, which has a quasi 2D crystal structure with $S=1/2$ Cu moments as shown in Figs. 1(a) and 1(b). The magnetic susceptibility χ of this system, shown in Fig. 2, exhibits typical spin-gap
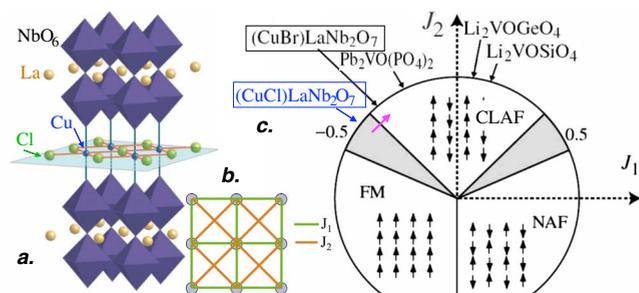

FIG. 1. (Color online) (a) Crystal structure of (CuCl)LaNb$_2$O$_7$ (Ref. 11). (b) Exchange interactions J_1 and J_2 on the 2D square lattice. (c) Conceptual phase diagram of the spin-1/2 square-lattice J_1-J_2 model (Refs. 12 and 13) as a function of J_1 and J_2 with regions of collinear antiferromagnetic (CLAF), ferromagnetic (FM) and Néel AF order. A spin-gap or spin-liquid state is expected in the shaded region. The present work elucidates the evolution illustrated by the purple arrow between the FM and CLAF phases.
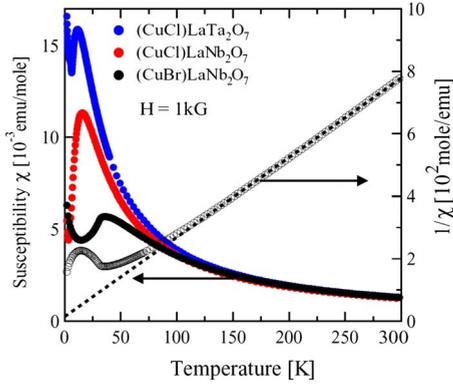
FIG. 2. (Color online) Magnetic susceptibility χ of (CuCl)LaNb$_2$O$_7$, (CuCl)LaTa$_2$O$_7$ and χ and $1/\chi$ of (CuBr)LaNb$_2$O$_7$ in an external field of 1 kG.

behavior with an estimated gap $\Delta/k_B = 27$ K. The spin gap was directly observed by inelastic neutron scattering[11] and high-field magnetization.[14] The very small Weiss temperature $\Theta = J_1 + J_2 \leq 5$ K in the $1/\chi$ plot (Fig. 2) indicates that J_1 and J_2 have nearly equal magnitudes but opposite signs. Based on these observations, we assign this compound to fall in the spin-gap region in Fig. 1(c).

A sister compound (CuBr)LaNb$_2$O$_7$ orders into a collinear antiferromagnet (CLAF) below $T_N = 32$ K, as shown by neutron-scattering[15] and susceptibility measurements (Fig. 2). This indicates a slight change in the J_2/J_1 ratio of the Br compound from that of the Cl compound [Fig. 1(c)], together with a relatively large magnitude of the antiferromagnetic J_2 which is at least enough to support this Néel temperature. In order to study the evolution from the CLAF to the spin-gap states, illustrated by a purple arrow in Fig. 1(c), we investigate solid solution systems Cu(Cl$_{1-x}$Br$_x$)LaNb$_2$O$_7$ as well as (CuCl)La(Nb$_{1-y}$Ta$_y$)$_2$O$_7$.[16] The latter substitution is of great interest since it tends to suppress the spin gap, as seen in χ for $y = 1$ in Fig. 2, without perturbing the direct exchange path on the CuCl square-lattice plane. This may allow finer tuning of the J_2/J_1 ratios with a smaller effect of randomness.

We started a project to study these systems by μSR in 2005. Since then a few parallel efforts have been made in neutron-scattering, high-field susceptibility/magnetization, NMR,[17] and Raman-scattering[18] measurements. Details of sample preparation, elastic neutron-scattering, and high-field magnetization/susceptibility studies will be reported by Tsujimoto *et al.*[19] for the (Cl,Br) substitution systems, and by Kitada *et al.*[20] for the (Nb,Ta) substitution systems. In this paper, we focus on μSR and low-field magnetic-susceptibility measurements on Cu(Cl,Br)La(Nb,Ta)$_2$O$_7$, which demonstrate: (a) absence of static magnetism in (CuCl)LaNb$_2$O$_7$ down to 15 mK confirming the spin-gapped ground state; (b) phase separation between partial volumes with a spin gap and static magnetism in (CuCl)La(Nb,Ta)$_2$O$_7$; (c) history-dependent magnetization in the (Nb,Ta) and (Cl,Br) substitution systems; and (d) a uniform long-range collinear antiferromagnetic state in (CuBr)LaNb$_2$O$_7$.

The development of theories for J_1-J_2 systems are in progress. Following initial conjecture[12,13] of existence of a spin gap in the border region of CLAF state and ferromagnetic (FM) state, a more recent theory[21] predicts nematic spin arrangement, instead of the spin gap, at this border, when first- and second-neighbor interactions are considered in a Heisenberg model of a two-dimensional square lattice. However, a spin-gap state could well be expected for situations involving higher-order interactions, such as, third- and fourth-nearest-neighbor exchange interactions, anisotropy or three-dimensional interlayer couplings. In a recent experimental effort to develop compounds relevant to the present Cu(Cl,Br)La(Nb,Ta)$_2$O$_7$ system, Tsujimoto *et al.*[22] synthesized (CuBr)A_2B_3O$_{10}$ (A=Ca,Sr,Ba,Pb; B=Nb,Ta) which has three perovskite layers between the adjacent CuBr planes. One of these systems, (CuBr)Sr$_2$Nb$_3$O$_{10}$, exhibits a positive Curie temperature when the high-temperature susceptibility χ is extrapolated to low temperatures in a plot of $1/\chi$ versus T. This suggests that a fine tuning of parameters indeed brings the square-lattice Cu(Cl,Br) plane into the side of FM correlations across the spin-gap region, as illustrated in Fig. 1(c).

In an NMR study of CuClLaNb$_2$O$_7$ Yoshida *et al.*[17] found a signature of dimerization, although the corresponding superlattice satellite peaks of x-ray scattering are rather weak in intensity, and the assigned symmetry is not fully consistent with the results of recent Raman measurements.[18] In view of these developments, here we adopt the J_1-J_2 model as an appropriate starting point for discussions of Cu(Cl,Br)La(Nb,Ta)$_2$O$_7$, although there may be some influence of higher-order interactions, dimerization, and other effects existing in real materials. Even when a small dimerization is essential for the formation of the spin gap, all the experimental results described in this paper can still be regarded as elucidating an interesting boundary between a spin-gap and CLAF state.

During the course of this study, we found a history dependence of the magnetic susceptibility of Cu(Cl,Br)La(Nb,Ta)$_2$O$_7$ which sets in at $T \sim 7$ K in a low applied field of ~ 100 G. This feature will be reported in Sec. IV, following the μSR results in Sec. III. A renewed interest in J_1-J_2 systems was generated by the recent discovery of La(F,O)FeAs superconductors[23] which have Fe moments in this geometry.[24,25] In Sec. V, we will compare the present results with μSR studies of other GFSS, including Kagomé lattice systems, cuprate and other systems on body-centered tetragonal lattices, and FeAs superconductors.

II. EXPERIMENTAL METHODS

Polycrystal specimens of solid solution systems Cu(Cl$_{1-x}$Br$_x$)LaNb$_2$O$_7$ and (CuCl)La(Nb$_{1-y}$Ta$_y$)$_2$O$_7$ (Ref. 16) were synthesized at Kyoto University using ion-exchange reactions at low temperatures, as described in Refs. 19 and 20. X-ray diffraction results show no trace of impurity phases for the entire concentration regions $0 \leq x \leq 1$ and $0 \leq y \leq 1$ within the experimental detection limit. In the case of (Cl,Br) substitutions, the homogeneous and random distribution of substituted atoms has been verified by the variation in the tetragonal a-axis and c-axis lattice constants against composition x (Ref. 19) following Vegard's law. For the

(Nb,Ta) substitutions, similar information could not be obtained from x-ray diffraction due to nearly equal atomic radius of Nb and Ta. Chemical homogeneity of both the (Br,Cl) and (Nb,Ta) samples have been checked using energy dispersive spectroscopy of transmission electron microscope measurements, which confirmed uniform solutions with the spatial resolution of 10 nm.[19,20] The specimens were pressed into disk-shaped pellets having typical dimensions of 10 mm in diameter and 1–2 mm in thickness. The magnetic susceptibility of a small piece of each of these specimens was measured using a standard Quantum Design superconducting quantum interference device magnetometer at Kyoto University.

μSR measurements were performed at TRIUMF, the Canadian National Accelerator Laboratory in Vancouver. Polarized positive muons were implanted one by one into the specimens mounted in a gas-flow He cryostat for measurements above $T=2.0$ K at the M20 or M15 channels and in a dilution-refrigerator cryostat for those between 15 mK and 10 K at the M15 channel. The time evolution $A(t)$ of the muon spin polarization was obtained from the time histograms $F(t)$ and $B(t)$ of the forward and backward counters as

$$A(t) = A_oG(t) = [F(t) - B(t)]/[F(t) + B(t)], \qquad (1)$$

where $G(t)$ represents the relaxation function defined with $G(0)=1$. Details of the μSR methods can be found in Refs. 3 and 4.

III. EXPERIMENTAL RESULTS: μSR

A. Zero-field μSR spectra: Ground state

Due to its superb sensitivity to static magnetic order in spin systems with random/dilute/very small ordered moments, μSR provides a very stringent test to verify the absence of active magnetism expected in spin-gap candidate systems.[26,27] Figure 3(a) shows the zero-field (ZF) μSR time spectra obtained for $(CuCl)LaNb_2O_7$ which exhibit a very slow relaxation at $T=2$ K and 15 mK. This depolarization can be decoupled by a small longitudinal field (LF) of 50 G. These features are expected for relaxation caused by static nuclear dipolar fields. To ensure good heat conduction at 15 mK, we reproduced the results with another ceramic specimen containing 30% Au powder by weight. Thus, we confirmed the absence of static magnetic order in $(Cu,Cl)LaNb_2O_7$ down to 15 mK. Statistical/systematic error of the measurement gives an upper limit of less than 2% of the total volume for the volume V_M with static magnetism.

In contrast, fast decay of the ZF-μSR spectra was observed at $T=1.8$ K in $(Nb_{1-y}Ta_y)$ substitution systems with $y \gtrsim 0.3$. With increasing y, the amplitude of the fast-relaxing component increases [Fig. 3(a)], indicating the existence of static magnetism with increasing volume fraction V_M. In the CLAF system $(CuBr)LaNb_2O_7$, ZF-μSR spectra $A(t)$ exhibit long-lived precession below T_N [Fig. 3(b)] which indicates the existence of a well-defined local field at the muon site expected for homogenous long-range order. With decreasing Br composition x in the $(Cl_{1-x}Br_x)$ substitution, the internal field at $T \sim 2$ K becomes increasingly inhomogeneous as

a.

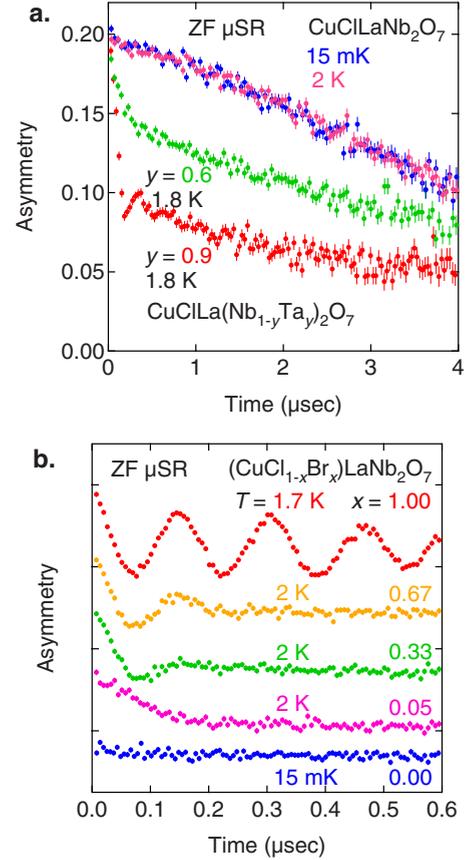**b.**

FIG. 3. (Color online) (a) ZF-μSR time spectra in $(CuCl)LaNb_2O_7$ demonstrating absence of static magnetism, and in $(CuCl)La(Nb_{1-y}Ta_y)_2O_7$ showing magnetic order in a partial volume fraction. (b) ZF-μSR spectra in $(CuCl_{1-x}Br_x)LaNb_2O_7$ at low temperatures.

shown by the damping of the oscillation in Fig. 3(b). For $x=0.05$, the inhomogeneous static local field results in a ZF-μSR line shape often seen in dilute alloy spin-glass systems.[28] The change in the initial damping rate in Fig. 3(b) between $x=0.33$ and 0.05 indicates that the spin structure/orientation or size and spatial uniformity of the ordered moment changes between these two concentrations. We confirmed a static origin of the observed fast relaxation in $x=0.05$ via decoupling in LF at $T=15$ mK.

B. Zero-field μSR spectra: Temperature dependence

Figure 4 shows the time spectra of ZF-μSR observed in $(CuBr)LaNb_2O_7$ and $(CuCl)LaTa_2O_7$ at several different temperatures. Coherent oscillations are observed in the signal below the Néel temperature $T_N=32$ K for the former and 7 K for the latter system. The spectra of $(CuBr)LaNb_2O_7$ fit well to

$$G_z(t) = A_1[\cos(\omega t)\exp(-\Lambda_1 t)] + A_2[\exp(-\Lambda_2 t)]$$
$$+ A_3[\exp(-\Lambda_3 t)], \qquad (2)$$

where the first term represents the oscillating component, the second term represents a component showing a fast damping with $\Lambda_2 \sim \omega$, and the third term represents a persisting slowly
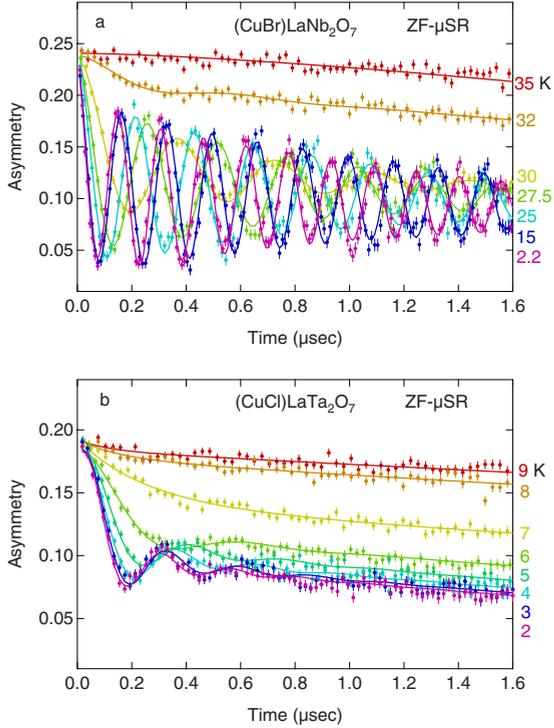
FIG. 4. (Color online) ZF-μSR time spectra in (a) (CuBr)LaNb$_2$O$_7$ and (b) (CuCl)LaTa$_2$O$_7$ showing the onset of long-range antiferromagnetic order. The solid lines represent Eq. (2) in (a) and Eq. (3) in (b).

relaxing signal with $\Lambda_3 \ll \omega$. The spectra of (CuCl)LaTa$_2$O$_7$ exhibit faster depolarization of the oscillation and fit well to a Bessel function term plus a nearly constant term,

$$G_z(t) = A_1[(1/\omega t)\sin(\omega t)\exp(-\Lambda_1 t)] + A_3[\exp(-\Lambda_3 t)]. \tag{3}$$

Previously, the Bessel function line shape was found in ZF-μSR spectra from systems having incommensurate spin-density wave[29] or stripe spin modulation.[4] Neutron-scattering measurements of (CuCl)LaTa$_2$O$_7$, however, found a commensurate CLAF state.[20] Thus the present results may simply be due to highly disordered short-range AF correlations.

In Fig. 5, we show the observed frequency $\nu = \omega/2\pi$ for the (Cl,Br) system with $x = 1.0$, 0.67, 0.33, and (CuCl)LaTa$_2$O$_7$. The spectra from the latter three systems were fit to Bessel functions, in view of significantly better fits as compared to the cosine function, although none of these systems exhibit a clear indication of incommensurate spin correlations in neutron scattering. With decreasing Br composition x, T_N decreases, but the frequency $\nu(T \rightarrow 0)$ remains nearly unchanged at $0.33 \leq x \leq 1$. This indicates that the size of the ordered Cu moment does not depend on x. The frequency $\nu(T \rightarrow 0)$ for (CuCl)LaTa$_2$O$_7$ is significantly different from that of the other systems in Fig. 5, despite the fact that the same ordered Cu moment size $\sim 0.6\mu_B$ was reported by neutron-scattering studies.[19,20] The lower frequency/internal field was also found in all the (Nb,Ta) systems with $0.3 \leq y \leq 1$ (as discussed later) as well as in the (Cl,Br) system with $x = 0.05$ [see Fig. 3(b)]. Interestingly,
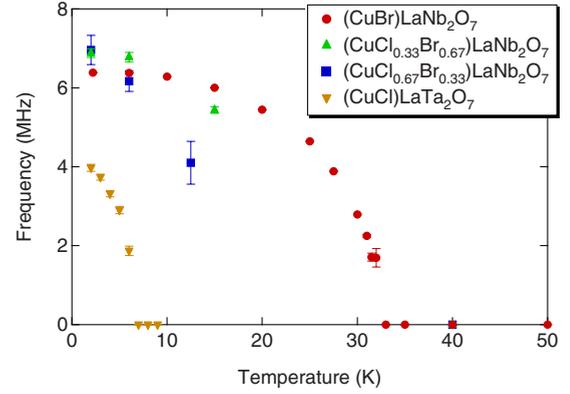

FIG. 5. (Color online) Muon spin precession frequency ν observed in Cu(Cl$_{1-x}$Br$_x$)LaNb$_2$O$_7$ with $x = 1.0$, 0.67, and 0.33, and in (CuCl)LaTa$_2$O$_7$

these systems with the lower internal field all have a Néel temperature of $T_N \sim 7$ K. These observations suggest that compounds with sufficiently reduced T_N have a short-ranged spin structure and a possibly different direction of the ordered Cu moments compared to systems with higher T_N.

C. Results in weak transverse field: Volume fraction of the magnetically ordered region

To determine the volume fractions of regions with and without static magnetic order, μSR measurements in weak transverse field (WTF) are quite useful, as shown in Ref. 3. The persistent oscillation amplitude in WTF reflects muons landing in a paramagnetic or nonmagnetic environment. Figures 6(a) and 6(b) show the precessing amplitudes in (Nb$_{1-y}$Ta$_y$) and (Cl$_{1-x}$Br$_x$) systems mostly in WTF = 100 G. Some of the data were obtained with WTF ~ 50 and 30 G due to limitation of available spectrometers. A sharp onset of the CLAF ordered state is seen for the Br substitutions with $x = 0.2-1$ [Fig. 6(b)] at temperatures consistent with the magnetic susceptibility results reported by Tsujimoto *et al.*[19] The (Nb,Ta) systems show static magnetism below a common onset temperature $T_N \sim 6-7$ K with the paramagnetic volume fraction decreasing gradually with decreasing temperature toward the partial fraction dependent on y. This confirms the phase separation observed in ZF-μSR.

In both Figs. 6(a) and 6(b), about 25% of muons remain in a paramagnetic environment even when static magnetism is established in the full volume fraction as in the CLAF state of (CuBr)LaNb$_2$O$_7$.[15] Approximately half of this signal can be ascribed to background muons, which missed the specimen and stopped in sample-holding films and/or a scintillation counter placed behind the specimen, subsequently escaping from the electronics veto mechanism. We calibrated this instrument-originated background[30] and show its level by the dotted lines in Fig. 6. At present, the exact origin of the other half of the backgroundlike signal is unknown. Conceivable scenarios include that these $\sim 10-15$ % of muons are occupying sites where local fields from antiferromagnetic Cu spins cancel for symmetry reasons. In the present work, we assume that they are not sensitive to magnetic order[31] and estimate the volume fraction V_M with static magnetic order
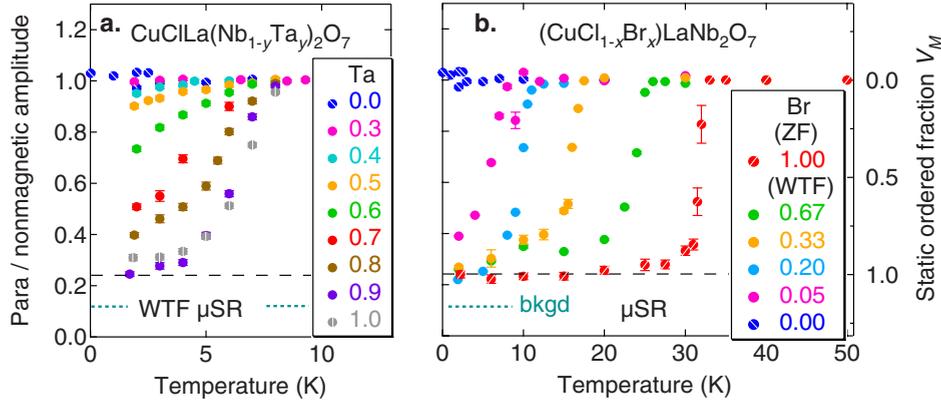
FIG. 6. (Color online) [(a) and (b)]: Amplitude of persisting muon spin precession in a WTF of 100 G in (a) (CuCl)La(Nb,Ta)$_2$O$_7$ and (b) Cu(Cl,Br)LaNb$_2$O$_7$. This represents the fraction of muons landing in paramagnetic or nonmagnetic environment. In each specimen, about 25% of the amplitude persists at any temperature and composition as denoted by the dashed lines. The dotted lines show the level of the background originating from instruments (Ref. 30).

as indicated by the right-side label of Fig. 6. Judging from the amplitude from the remaining 75% of muons, we thus conclude that systems with $x \geq 0.2$ order in a full volume fraction $V_M = 1.0$, while those with $0.3 \leq y < 0.9$ undergo phase separation between ordered and spin-gapped volumes. The spin-gap volume prevails to nearly the full fraction for $y < 0.3$. The ambiguity related to the small backgroundlike signal would not alter the essential features of these conclusions.

D. ZF-μSR spectra in phase-separated systems

Static magnetism in the phase-separated region can be elucidated by ZF-μSR spectra in Figs. 7(a) and 7(b) for quantum [Fig. 7(a)] and thermal [Fig. 7(b)] evolution in the (Nb,Ta) systems. The similarities of these two figures demonstrates that near the phase boundary between CLAF and spin-gapped states, both quantum and thermal transitions involve phase separation with gradual change in V_M as a function of temperature T and composition y. These spectra can be decomposed into two components with fast and slow re-

laxation, having T- and y-dependent amplitude ratios, respectively. The exponential relaxation rate Λ of the fast component is nearly independent of T and y, as shown in Fig. 7(c), which implies that the ordered regions in different T and y share common microscopic spin arrangements of Cu moments. The common decay rate, indicative of the same spin configuration, is also found in the $x = 0.05$ (Br,Cl) substitution system [Fig. 2(c)]. The present experiment, however, does not allow us to estimate the typical size of the ordered regions.

IV. EXPERIMENTAL RESULTS: LOW-FIELD MAGNETIC SUSCEPTIBILITY

Motivated by the ZF-μSR line shapes in Fig. 7 which resemble those expected in spin-glass systems,[28] we performed measurements of dc-magnetization M in a weak field of 100 G with both field cooling (FC) and zero-field cooling (ZFC), by using small pieces of specimens cutoff from those used in the present μSR measurements [solid symbols in Figs. 8(a) and 8(b)]. As shown in Fig. 8(a), marked departure
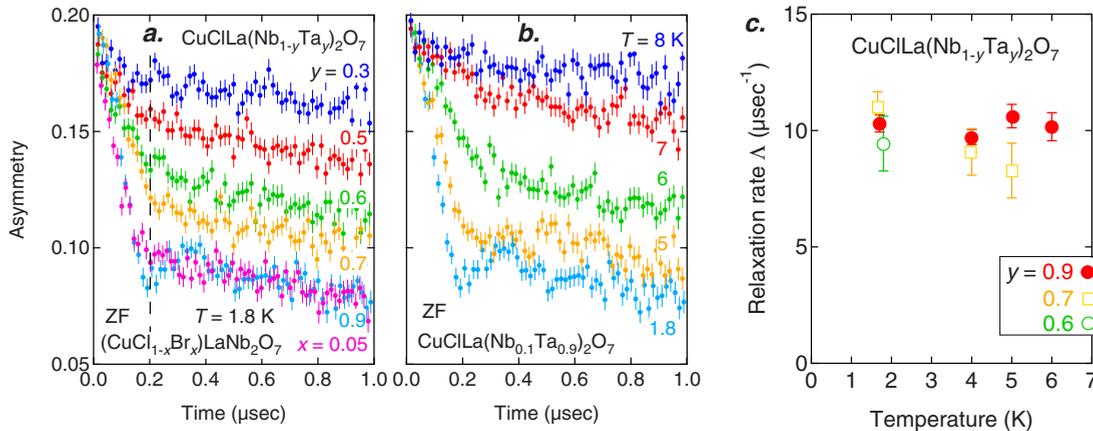

FIG. 7. (Color online) (a) System and (b) temperature dependence of the μSR time spectra in zero field in (CuCl)La(Nb,Ta)$_2$O$_7$, which exhibit signals of fast- and slow-decay components, with composition- and T-dependent amplitudes. (c) The exponential muon spin relaxation rate Λ of the fast decay component in (a) and (b).
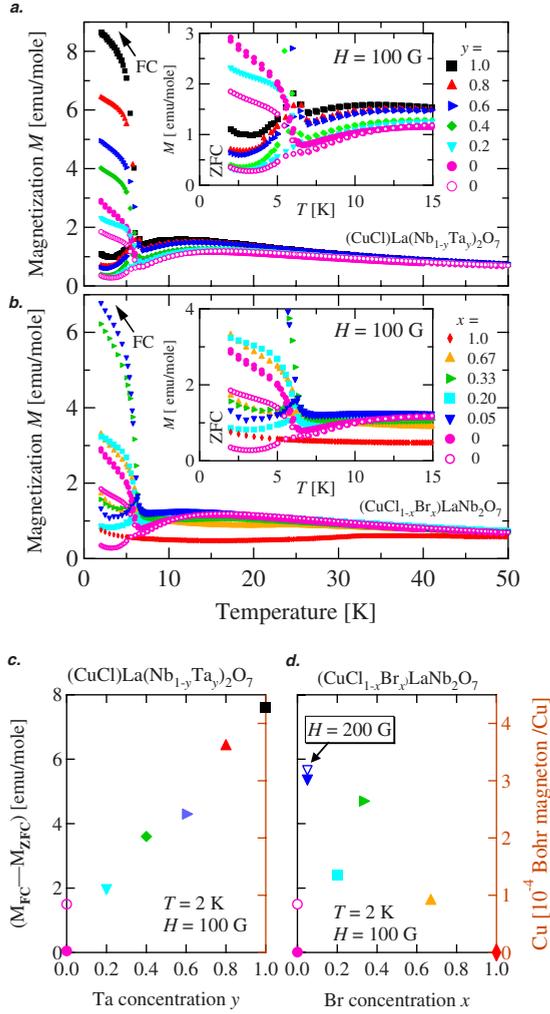
a.

b.

c. (CuCl)La(Nb$_{1-y}$Ta$_y$)$_2$O$_7$

d. (CuCl$_{1-x}$Br$_x$)LaNb$_2$O$_7$

FIG. 8. (Color online) [(a) and (b)] Magnetic susceptibility for both FC and ZFC in 100 G obtained in (a) (CuCl)La(Nb,Ta)$_2$O$_7$ and (b) Cu(Cl,Br)LaNb$_2$O$_7$. [(c) and (d)] The irreversible magnetization $M_{irr} \equiv M_{FC} - M_{ZFC}$ at $T = 2$ K. For (CuCl)LaNb$_2$O$_7$ (i.e., $y = 0$ and $x = 0$), results from two different specimens are shown: sample (I) (open circles) which was used in the high-field magnetization studies (Ref. 20), and sample (II) (closed circles) which was used in the present μSR measurements. The inset of (b) shows that M_{ZFC} and M_{FC} of sample (II) increase below $T \sim 6$ K without significant irreversibility effect. In (d), we also added a point of M_{irr} for the $x = 0.05$ (Cl,Br) system obtained in $H = 200$ G. Nearly identical values of M_{irr} for $H = 100$ and 200 G indicate a static origin of the irreversible magnetization.

of M_{FC} from M_{ZFC} sets in at $T = 6$ K, coinciding with the onset of static magnetism in the (Nb$_{1-y}$Ta$_y$) systems. History dependence of M was also found in (Cl$_{1-x}$Br$_x$) systems with $x \leq 0.66$, with a common onset temperature of 6 K, well below T_N for $x = 0.66$, 0.33, and 0.2 [Fig. 8(b)]. The magnitudes of $(M_{FC} - M_{ZFC})$ at $T = 2$ K for all of these systems correspond to a very small ferromagnetic polarization $\leq 10^{-3} \mu_B$ per Cu [Figs. 8(c) and 8(d)], nearly independent of the field for the FC measurements in 100–800 G in the $x = 0.05$ system [Fig. 8(d)].

The irreversible magnetization $M_{irr} \equiv (M_{FC} - M_{ZFC})$ in (CuCl)La(Nb$_{1-y}$Ta$_y$)$_2$O$_7$ at $T = 2$ K [Fig. 8(a)] roughly scales

with the volume fraction V_M of the magnetically ordered region [Fig. 6(a)]. M_{irr} and V_M share the same onset temperature. These features suggest that the observed signal likely comes from the bulk volume of the region with static magnetism, rather than from dilute ferromagnetic impurities. The very small net ferromagnetic polarization [Figs. 8(c) and 8(d)], together with the static Cu moment size of $\sim 0.6\mu_B$, indicate mostly antiferromagnetic or random spin configurations, with a very small ferrimagnetic/canted component. Without distinguishing between these, we term the static magnetism in the (Nb,Ta) system as a "glassy antiferromagnetic" (GAF) state. The relatively large M_{irr} observed in the $y = 1$ pure Ta material rules out the notion that the irreversibility requires randomness and/or a nonstoichiometric solid solution. Figures 8(c) and 8(d) show comparable magnitudes of M_{irr} for the $y = 0.8 - 1.0$ (Nb,Ta) systems and $x = 0.05$ (Cl,Br) system. This feature corresponds well to the nearly identical ZF-μSR spectra observed in the $y = 0.9$ (Nb,Ta) and $x = 0.05$ (Cl,Br) systems shown in Fig. 7(a).

For the unsubstituted (CuCl)LaNb$_2$O$_7$, we included the magnetization results from two specimens in Fig. 8; one used in the high-field magnetization studies[20] (open circle; sample I) and the other used in the present μSR studies (closed circle; sample II). The μSR sample (II) showed nearly zero M_{irr}, consistent with the absence of static magnetism found by μSR. Small, yet somewhat surprising nonzero values of M_{irr} in the $y = 0.2$ system may be due to increasing ferrimagnetic/canted contributions, possibly from remaining static regions with a volume fraction $\leq 2\%$, which was not detected by μSR. The nonzero M_{irr} for the $y = 0$ sample (I) may be caused by a similar situation.

V. PHASE DIAGRAM

Summarizing these findings, we present a phase diagram in Fig. 9 as functions of the substitution concentrations x and y. The phase-separated region with a partial volume fraction is illustrated by a striped pattern while regions with a full volume fraction are indicated by solid colors. The first-order thermal transition is shown by the broken line while the solid line indicates the transitions which are likely second order. The internal field observed in the CLAF state (pink) is significantly larger than that in the GAF state (green), suggesting that these states are distinct. Further characterization is required to clarify the coexistence of these two states in the region of $0.05 \leq x \leq 1$. The purple and orange arrows indicate, respectively, the history dependent region (HD) where $M_{FC} \neq M_{ZFC}$ and the region with phase-separated static magnetism in a partial volume fraction (PV).

VI. DISCUSSION

The present μSR results have demonstrated that (CuCl)LaNb$_2$O$_7$ indeed possesses a nonmagnetic ground state, consistent with spin-gap formation, over the full volume fraction. μSR has a superb sensitivity to static magnetism, as even small nuclear dipolar fields can easily be detected. The present study established the absence of any detectable static and dynamic magnetism from Cu moments,
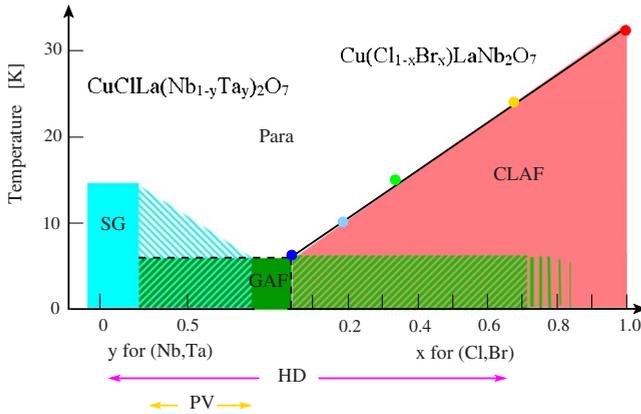
FIG. 9. (Color online) Phase diagram of $Cu(Cl,Br)La(Nb,Ta)_2O_7$ obtained in the present study, with spin-gap (SG), glassy antiferromagnetic (GAF), and collinear antiferromagnetic (CLAF) states. The striped region indicates phase separation. The broken and solid lines denote, respectively, first- and second-order thermal transitions. The arrows attached to the horizontal axis show the region with history dependence (HD) of the magnetic susceptibility and the region where static magnetism exists in a partial volume fraction (PV).

and demonstrated that the gapped state in $(CuCl)LaNb_2O_7$ is really robust. Our results also revealed phase separation between volumes with and without static magnetism in $(CuCl)La(Nb_{1-y}Ta_y)_2O_7$ for the Ta concentration $y > 0.3$. Kitada et al.[20] report neutron-scattering results of the (Nb,Ta) systems, where the volume fraction was estimated from the intensities of the magnetic Bragg peaks. They also decomposed the response of high-field magnetization into the "gapped" and "ungapped" signals, using the results of the $y = 0.4$ compound as the reference for the former and $y = 1$ for the latter, and estimated the volume fraction of the ungapped signal. The volume fraction values derived from the neutron and magnetization results in these procedures agree well with V_M from μSR.

Both neutron and magnetization studies detect magnetism as a volume-integrated quantity, and they cannot distinguish a small volume with a large individual moment versus a large volume with a small moment. In contrast, μSR and NMR produce distinguishable signals from magnetically ordered and paramagnetic regions, with the amplitudes proportional to corresponding volumes: the volume information is decoupled from that of the moment size. Consequently, the real-space probes μSR and NMR have genuine advantages over neutron and magnetization in the determination of ordered volume fractions. In the present (Nb,Ta) systems, the size of the ordered moment does not depend on the Ta concentration y, as demonstrated in Fig. 7. Due to this feature, the neutron and magnetization results for the volume fraction agreed well with the μSR results.

From signatures in the magnetic susceptibility for the (Cl,Br) systems, Tsujimoto et al.[19] derived the Néel temperatures which are quantitatively consistent with the present μSR results. Since the positive muon is a charged probe, there remains some suspicion that the μSR results may be different from those of the bulk system due to possible perturbation caused by the presence of the muon. The good

agreements of the volume fraction and T_N with the neutron and susceptibility/magnetization results confirm that the muons are indeed probing bulk properties in the present systems. The μSR results in Fig. 3(b) indicate increasingly short-ranged spin correlations with decreasing Br concentration x. This feature was not detected by neutrons, presumably due to limited instrumental resolution and the weak signal expected from the magnetic Bragg reflections for powder specimens. The spin correlation length remains to be determined by neutron studies in the future using single-crystal specimens.

History dependence of the magnetization M has also been observed in the Kagomé lattice antiferromagnets $SrCr_xGa_{12-x}O_{19}$ (SCGO),[32] Cr-jarosite,[33] and many other GFSS, but without a jump in M_{FC} at the onset temperature. The M_{FC} jump observed in the present J_1-J_2 systems may be related to the involvement of the ferromagnetic exchange interaction J_1, which does not exist in other GFSS based exclusively on antiferromagnetic couplings. The partial volume fraction of the magnetically ordered region adjacent to the spin-singlet region has also been observed recently by μSR studies in the Kagomé lattice Herbertsmithite system $Zn_xCu_{4-x}(OH)_6Cl_2$ in a quantum evolution with the Zn concentration x as a tuning parameter.[26] Figure 10 shows a schematic view of free-energy variation. A free-energy profile with multiple minima at the order-parameter (m) values of zero and a finite value in Fig. 10 (lines c and d) can explain the origin of a first-order transition which often results in phase separation. History dependence can be caused by multiple free-energy minima, as generally seen in spin glasses with complicated free-energy landscapes with many minima. The present results show, however, that the regions for these two phenomena (purple and orange lines in Fig. 9) do not completely overlap.

When we look into previous μSR and susceptibility results in frustrated spin systems, we notice three patterns: (a) spin freezing at T_g, associated with critical slowing down (maxima of $1/T_1$ of μSR), history dependence of M below T_g, and disappearance of dynamics at $T \rightarrow 0$: canonical spin glasses AuFe, CuMn,[28] and AgMn.[34] (b) Slowing down of
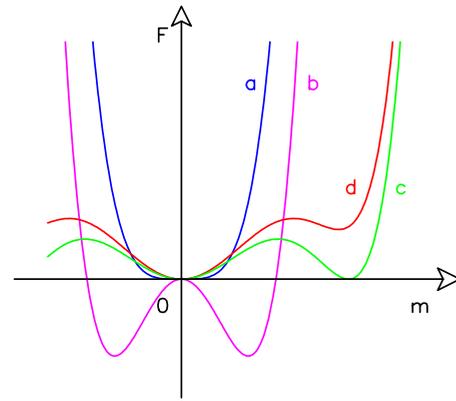

FIG. 10. (Color online) A schematic view of free-energy profile as a function of magnetic order parameter m. The curves (a) and (b) represent the case of standard second-order phase transitions, above and below T_c, respectively, while (d) and (c) for the first-order transitions with (d) above T_c and (c) at T_c.

spin fluctuations toward T_g, history dependence of M below T_g, followed by persistent dynamic effects at $T \rightarrow 0$, M remaining finite at $T \rightarrow 0$: Kagomé lattice systems SCGO $SrCr_8Ga_4O_{19}$,[35] Cr-jarosite $KCr_3(OH)_6(SO_4)_2$,[33] and volborthite $(Cu_xZn_{1-x})_3V_2O_7(OH_2)2H_2O$,[36,37] and a body-centered-tetragonal system $CePt_2Sn_2$.[38] (c) Spatially uniform ground state without static or dynamic magnetism at $T \rightarrow 0$ associated with clear reduction in M at $T \rightarrow 0$ which suggests a formation of spin gap in the unperturbed system, and appearance of phase-separated static magnetism when composition is varied: $(CuCl)LaNb_2O_7$ and the Kagomé system Herbertsmithite $Zn_xCu_{4-x}(OH)_6Cl_2$.[26,39,40]

We also note that a doped Haldane gap system $(Y,Ca)_2BaNiO_5$ (Ref. [41]) exhibits responses of the pattern (b) while the results of cuprate[4,5] and FeAs superconductors[42,43] correspond to the pattern (c). These observations suggest that near the fully spin-gapped (nonmagnetic and/or superconducting) state, systems have two choices: either to phase separate and exhibit magnetic order in a partial volume fraction [pattern (c)] or to become a strange "spin liquid" that shows persistent dynamic spin responses at $T \rightarrow 0$ in the whole volume [pattern (b)].

Recent μSR results in MnSi and $(Sr,Ca)RuO_3$ (Ref. [3]) revealed phase separation at QPTs, very similar to the present results. Some history dependence was also noticed in MnSi (Ref. [44]) near the phase boundary where static mag-

netism disappears. Phase separation in high Tc cuprates was observed in the QPT between spin-charge stripe and superconducting states,[4–6] and phase diagrams of many novel superconductors involve either first-order quantum evolution and/or phase separation.[45–47] Together with the present results, these accumulated results suggest importance of first-order phase transitions in physics of correlated electron systems. Comprehensive theoretical studies on this aspect may reveal further fascinating features.

*Authors to whom correspondence should be addressed.

[1] C. Pfleiderer, G. J. McMullan, S. R. Julian, and G. G. Lonzarich, Phys. Rev. B **55**, 8330 (1997).

[2] C. Pfleiderer, D. Reznik, L. Pintschovius, H. v. Löhneysen, M. Garst, and A. Rosch, Nature (London) **427**, 227 (2004).

[3] Y. J. Uemura, T. Goko, I. M. Gat-Malureanu, J. P. Carlo, P. L. Russo, A. T. Savici, A. Aczel, G. J. MacDougall, J. A. Rodriguez, G. M. Luke, S. R. Dunsiger, A. McCollam, J. Arai, Ch. Pfleiderer, P. Böni, K. Yoshimura, E. Baggio-Saitovitch, M. B. Fontes, J. Larrea, Y. V. Sushko, and J. Sereni, Nat. Phys. **3**, 29 (2007).

[4] A. T. Savici, Y. Fudamoto, I. M. Gat, T. Ito, M. I. Larkin, Y. J. Uemura, G. M. Luke, K. M. Kojima, Y. S. Lee, M. A. Kastner, R. J. Birgeneau, and K. Yamada, Phys. Rev. B **66**, 014524 (2002).

[5] K. M. Kojima, S. Uchida, Y. Fudamoto, I. M. Gat, M. I. Larkin, Y. J. Uemura, and G. M. Luke, Physica B (Amsterdam) **326**, 316 (2003).

[6] H. E. Mohottala, B. O. Wells, J. I. Budnick, W. A. Hines, Ch. Niedermayer, L. Udby, C. Bernhardt, A. R. Moodenbaugh, and F.-C. Chou, Nature Mater. **5**, 377 (2006).

[7] P. Schiffer and A. P. Ramirez, Comments Condens. Matter Phys. **18**, 21 (1996).

[8] G. Misguich and C. Lhuillier, in *Frustrated Spin Systems*, edited by H. T. Diep (World Scientific, Singapore, 2004).

[9] R. Melzi, P. Carretta, A. Lascialfari, M. Mambrini, M. Troyer, P. Millet, and F. Mila, Phys. Rev. Lett. **85**, 1318 (2000).

[10] E. E. Kaul, H. Rosnera, N. Shannon, R. V. Shpanchenkoc, and C. Geibel, J. Magn. Magn. Mater. **272-276**, 922 (2004).

[11] H. Kageyama, T. Kitano, N. Oba, M. Nishi, S. Nagai, K. Hirota, L. Viciu, J. B. Wiley, J. Yasuda, Y. Baba, Y. Ajiro, and K. Yoshimura, J. Phys. Soc. Jpn. **74**, 1702 (2005).

[12] N. Shannon, B. Schmidt, K. Penc, and P. Thalmeier, Eur. Phys. J. B **38**, 599 (2004).

[13] B. Schmidt, P. Thalmeier, and N. Shannon, Phys. Rev. B **76**, 125113 (2007).

[14] H. Kageyama, J. Yasuda, T. Kitano, K. Totsuka, Y. Narumi, M. Hagiwara, K. Kindo, Y. Baba, N. Oba, Y. Ajiro, and K. Yoshimura, J. Phys. Soc. Jpn. **74**, 3155 (2005).

[15] N. Oba, H. Kageyama, T. Kitano, J. Yasuda, Y. Baba, M. Nishi, K. Hirota, Y. Narumi, M. Hagiwara, K. Kindo, T. Saito, Y. Ajiro, and K. Yoshimura, J. Phys. Soc. Jpn. **75**, 113601 (2006).

[16] H. Kageyama, T. Kitano, R. Nakanishi, J. Yasuda, N. Oba, Y. Baba, M. Nishi, Y. Ueda, Y. Ajiro, and K. Yoshimura, Prog. Theor. Phys. Suppl. **159**, 39 (2005).

[17] M. Yoshida, N. Ogata, M. Takigawa, J. Yamaura, M. Ichihara, T. Kitano, H. Kageyama, Y. Ajiro, and K. Yoshimura, J. Phys. Soc. Jpn. **76** 104703 (2007).

[18] P. Lemmens, H. Kageyama *et al.* (unpublished).

[19] Y. Tsujimoto, A. Kitada, H. Kageyama, M. Nishi, K. Ohoyama, Y. Narumi, K. Kindo, Y. Kikuchi, Y. Ueda, Y. Ajiro, and H. Kageyama, arXiv:0.5103, J. Phys. Soc. Jpn. (to be published).

[20] A. Kitada, Y. Tsujimoto, H. Kageyama, Y. Ajiro, M. Nishi, Y. Narumi, K. Kindo, M. Ichihara, Y. Ueda, Y. J. Uemura, and K. Yoshimura, following paper, Phys. Rev. B **80**, 174409 (2009).

[21] N. Shannon, T. Momoi, and Ph. Sindzingre, Phys. Rev. Lett. **96**,

027213 (2006).

[22] Y. Tsujimoto, H. Kageyama, Y. Baba, A. Kitada, T. Yamamoto, Y. Narumi, K. Kindo, M. Nishi, J. P. Carlo, A. A. Aczel, T. J. Williams, T. Goko, G. M. Luke, Y. J. Uemura, Y. Ueda, Y. Ajiro, and K. Yoshimura, Phys. Rev. B **78**, 214410 (2008).

[23] Y. Kamihara, T. Watanabe, M. Hirano, and H. Hosono, J. Am. Chem. Soc. **130**, 3296 (2008).

[24] C. de la Cruz, Q. Huang, J. W. Lynn, J. Li, W. Ratcliff II, J. L. Zarensky, H. A. Mook, G. F. Chen, J. L. Luo, N. L. Wang, and P. Dai, Nature (London) **453**, 899 (2008).

[25] T. Yildirim, Phys. Rev. Lett. **101**, 057010 (2008).

[26] P. Mendels, F. Bert, M. A. de Vries, A. Olariu, A. Harrison, F. Duc, J. C. Trombe, J. S. Lord, A. Amato, and C. Baines, Phys. Rev. Lett. **98**, 077204 (2007).

[27] G. J. MacDougall, A. A. Aczel, J. P. Carlo, T. Ito, J. Rodriguez, P. L. Russo, Y. J. Uemura, S. Wakimoto, and G. M. Luke, Phys. Rev. Lett. **101**, 017001 (2008).

[28] Y. J. Uemura, T. Yamazaki, D. R. Harshman, M. Senba, and E. J. Ansaldo, Phys. Rev. B **31**, 546 (1985).

[29] L. P. Le, A. Keren, G. M. Luke, B. J. Sternlieb, W. D. Wu, Y. J. Uemura, J. H. Brewer, T. M. Riseman, R. V. Upasani, L. Y. Chiang, W. Kang, P. M. Chaikin, T. Csiba, and G. Gruner, Phys. Rev. B **48**, 7284 (1993).

[30] To calibrate the level of signals from muons that landed in the sample-supporting films and in the scintillation counter placed behind the specimen, which subsequently escaped from the electronics veto mechanism, we performed additional μSR measurements in a WTF$=100$ G using a specimen of a strong antiferromagnet SrFeO$_2$ ($T_N \sim 473$ K) (Ref. [48]) which has approximately the same dimensions (disc of 6 mm in diameter and 1–2 mm thick) as the present specimens of Cu(Cl,Br)La(Nb,Ta)$_2$O$_7$. At $T=3.5$ K, well below T_c, we observed the WTF amplitude of 0.022(1), which corresponds to about 10% of the total initial asymmetry. This result provides an estimate for backgroundlike signals originating from muons which missed the specimen. The dotted lines of Fig. 6 show the level of this background due to instruments.

[31] With this assumption, we obtain nearly full volume fraction of regions with static magnetic order for (CuBr)LaNb$_2$O$_7$ and (CuCl)LaTa$_2$O$_7$ below T_N. No signature of spin-gapped region in these unsubstituted systems was found by the neutron and magnetization studies published in Refs. [15], [19], and [20]. The magnetic volume fraction derived from the present μSR results in Fig. 6 for the (Nb,Ta) substitution systems is quantitatively consistent with the estimate from the neutron and magnetization studies in Ref. [20]. These consistencies with other results support our assumption that the $\sim 25\%$ of muons, indicated by the dashed lines in Fig. 6, are not sensitive to static magnetic order.

[32] A. P. Ramirez, G. P. Espinosa, and A. S. Cooper, Phys. Rev. Lett. **64**, 2070 (1990).

[33] A. Keren, K. Kojima, L. P. Le, G. M. Luke, W. D. Wu, Y. J. Uemura, M. Takano, H. Dabkowska, and M. J. P. Gingras, Phys. Rev. B **53**, 6451 (1996).

[34] R. H. Heffner, M. Leon, M. E. Schillaci, D. E. MacLaughlin, and S. A. Dodds, J. Appl. Phys. **53**, 2174 (1982).

[35] Y. J. Uemura, A. Keren, K. Kojima, L. P. Le, G. M. Luke, W. D. Wu, Y. Ajiro, T. Asano, Y. Kuriyama, M. Mekata, H. Kikuchi, and K. Kakurai, Phys. Rev. Lett. **73**, 3306 (1994).

[36] A. Fukaya, Y. Fudamoto, I. M. Gat, T. Ito, M. I. Larkin, A. T. Savici, Y. J. Uemura, P. P. Kyriakou, G. M. Luke, M. T. Rovers, K. M. Kojima, A. Keren, M. Hanawa, and Z. Hiroi, Phys. Rev. Lett. **91**, 207603 (2003).

[37] F. Bert, D. Bono, P. Mendels, J. C. Trombe, P. Millet, A. Amato, C. Baines, and A. Hillier, J. Phys.: Condens. Matter **16**, S829 (2004).

[38] G. M. Luke, A. Keren, K. M. Kojima, L. P. Le, W. D. Wu, Y. J. Uemura, G. M. Kalvius, A. Kratzer, G. Nakamoto, T. Takabatake, and M. Ishikawa, Physica B (Amsterdam) **206-207**, 222 (1995); G. M. Luke, K. Kojima, M. Larkin, J. Merrin, B. Nachumi, Y. J. Uemura, G. M. Kalvius, A. Brückl, K. Neumaier, K. Andres, G. Nakamoto, M. Sirasi, H. Tanaka, T. Takabatake, H. Fujii, and M. Ishikawa, Hyperfine Interact. **104**, 199 (1997).

[39] S. H. Lee, H. Kikuchi, Y. Qui, B. Lake, Q. Huang, K. Habicht, and K. Kiefer, Nature Mater. **6**, 853 (2007).

[40] In inelastic neutron-scattering measurements, a clear spin gap was observed in (CuCl)LaNb$_2$O$_7$ (Ref. [11]) while a clear gap signal was missing in ZnCu$_3$(OD)$_6$Cl$_2$ (Ref. [39]). Thus the former system may be characterized by a "dimer"-like local singlet while the latter by a more extended many-body singlet state.

[41] K. Kojima, A. Keren, L. P. Le, G. M. Luke, B. Nachumi, W. D. Wu, Y. J. Uemura, K. Kiyono, S. Miyasaka, H. Takagi, and S. Uchida, Phys. Rev. Lett. **74**, 3471 (1995).

[42] T. Goko, A. A. Aczel, E. Baggio-Saitovitch, S. L. Budko, P. C. Canfield, J. P. Carlo, G. F. Chen, P. C. Dai, A. C. Hamann, W. Z. Hu, H. Kageyama, G. M. Luke, J. L. Luo, B. Nachumi, N. Ni, D. Reznik, D. R. Sanchez-Candela, A. T. Savici, K. J. Sikes, N. L. Wang, C. R. Wiebe, T. J. Williams, T. Yamamoto, W. Yu, and Y. J. Uemura, Phys. Rev. B **80**, 024508 (2009).

[43] A. J. Drew, Ch. Niedermayer, P. J. Baker, F. L. Pratt, S. J. Blundell, T. Lancaster, R. H. Liu, G. Wu, X. H. Chen, I. Watanabe, V. K. Malik, A. Dubroka, M. Roessle, K. W. Kim, C. Baines, and C. Bernhard, Nature Mater. **8**, 310 (2009).

[44] C. Pfleiderer, D. Reznik, L. Pintschovius, and J. Haug, Phys. Rev. Lett. **99**, 156406 (2007).

[45] Y. J. Uemura, Nature Mater. **8**, 253 (2009).

[46] Y. J. Uemura, Physica B (Amsterdam) **404**, 3195 (2009).

[47] Y. J. Uemura, Physica B (Amsterdam) **374-375**, 1 (2006).

[48] Y. Tsujimoto, C. Tassel, N. Hayashi, T. Watanabe, H. Kageyama, K. Yoshimura, M. Takano, M. Ceretti, C. Ritter, and W. Paulus, Nature (London) **450**, 1062 (2007).